

## CHAPTER 11: SPATIAL DATA

So far we have concentrated on longitudinal data; we now consider spatial data. Two important distinctions are between lattice and non-lattice data. and between point data, and data aggregated over space.

Pure spatial data are fundamentally different from longitudinal data from multiple individuals, since they are a single realization. In this sense they are closer to time series data, though such data are often regularly spaced (which under assumptions of stationarity allows simplification of estimation), whereas with spatial data it is usual to have non-lattice data.

This lack of replication aspect of non-lattice data dictates that sandwich estimation is not available. Hence we concentrate on likelihood-based methods. Space-time data do offer replication.

347

### Motivating Examples

#### Example: Zinc levels in the Netherlands

This data set gives locations and top soil heavy metal concentrations (in ppm), along with a number of soil and landscape variables, collected in a flood plain of the river Meuse, near the village Stein in the South of the Netherlands.

Heavy metal concentrations are bulk sampled from an area of approximately  $15m \times 15m$ .

We may be interest in modeling the concentrations as a function of covariates (spatial regression), or predicting the concentration surface, which requires modeling the residual surface.

348

R code for analysis of the zinc data, using the **GeoR** package:

```
> library(geoR)
> data(meuse)
> zmat <- matrix(cbind(meuse$x,meuse$y,log(meuse$zinc)),
                 ncol=3,nrow=155,byrow=F)
> geozinc <- as.geodata(zmat,coords.col=c(1,2),data.col=c(3))
> plot(geozinc)
```

Figures 40 and 41 were created using the following code.

```
> cloudzinc <- variog(geozinc,option="cloud")
> plot(cloudzinc)
> binzinc0 <- variog(geozinc,uvec=seq(0,5000,250))
> plot(binzinc0)
```

349

2008 Jon Wakefield, Stat/Biostat 571

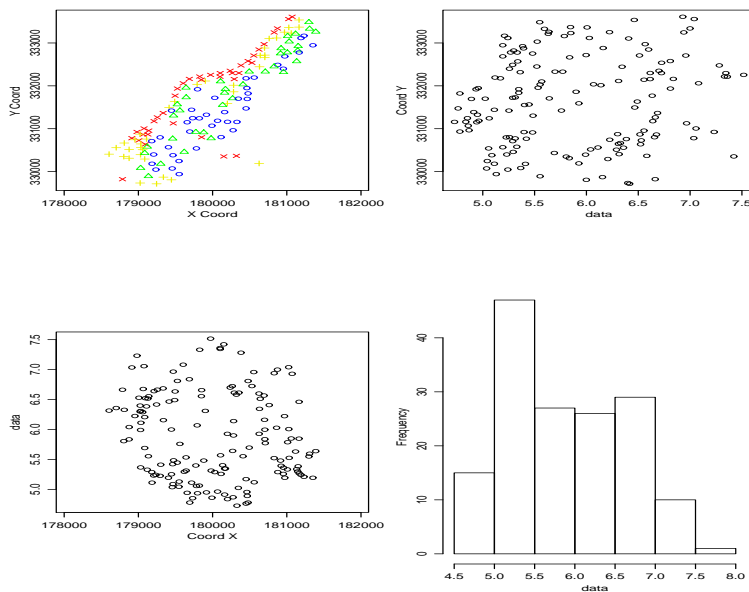


Figure 39: Exploratory plots for log zinc.

350

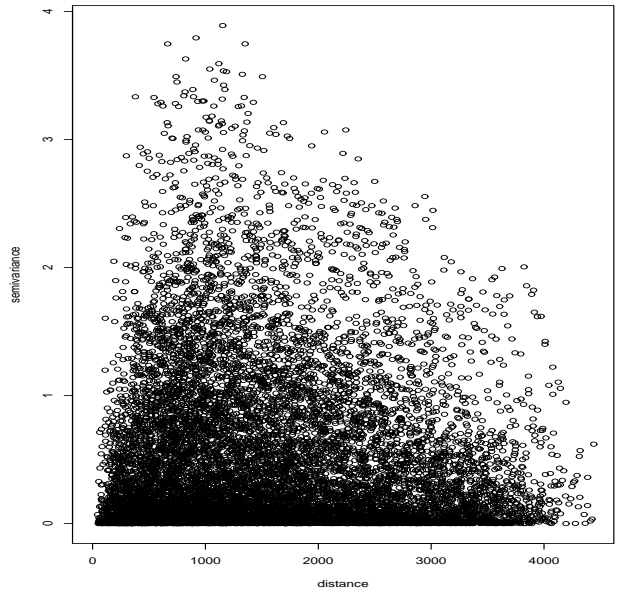


Figure 40: Variogram cloud for the log zinc data.

351

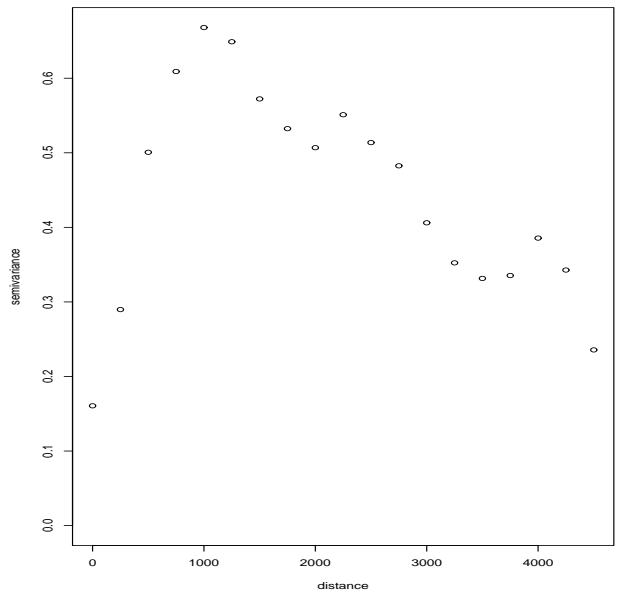


Figure 41: Binned variogram for the log zinc data.

352

## Childhood Asthma in Anchorage, Alaska

Study details:

- Study PI is Dr Mary Gordian. Data were collected on first grade children in Anchorage, with questionnaires being sent to the parents of children in 13 school districts (the return rate was 70% which has implications for interpretation).
- We analyze data on 905 children, with 885 between the ages of 5 and 7. There were 804 children without asthma, and 101 with asthma.
- The exposure of interest is exposure to pollution from traffic. Traffic counts were recorded at roads throughout the study region and a 50m buffer was created at the nearest intersection to the child's residential address and within this buffer traffic counts were aggregated (for confidentiality reasons the exact locations were not asked for in the survey).

Figure 42 shows the residential location of the cases and non-cases in Anchorage.

353

2008 Jon Wakefield, Stat/Biostat 571

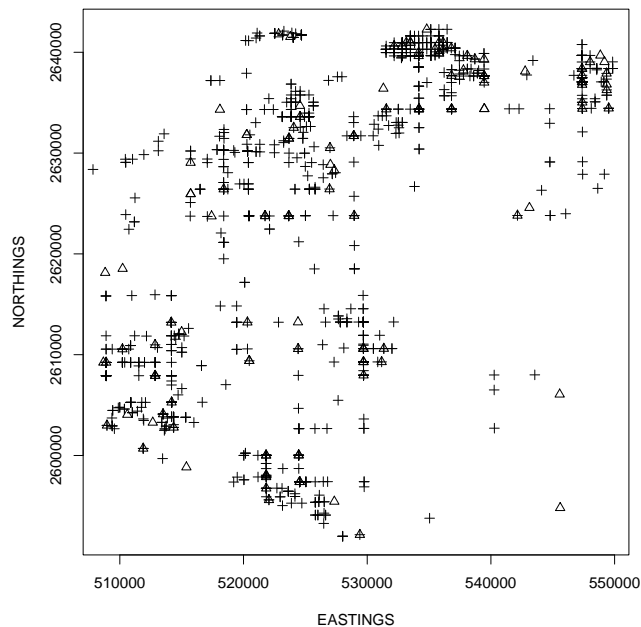


Figure 42: Asthma cases ( $\Delta$ ) and non-cases (+) in Anchorage.

354

*Naive non-spatial logistic modeling*

- Initially we may ignore confounding and the spatial nature of the data and fit a logistic regression of asthma incidence on exposure (with the exposure variable scaled to lie between 0 and 10).
- Such an analysis gives an odds ratio of 1.09 with a 90% confidence interval of 1.00–1.18.
- This analysis assumes that, given exposure, the Bernoulli 0/1 labels are independent. Due to unmeasured variables with spatial structure this is dubious and will result in inappropriate standard errors.

355

*Scottish Lip Cancer Data*

Incidence rates of lip cancer in males in 56 counties of Scotland, registered in 1975–1980. These data were originally reported in the mapping atlas of Kemp, Boyle, Smans and Muir (1985).

The form of the data is:

- Observed and expected number of cases (based on the county age populations),
- A covariate measuring the proportion of the population engaged in agriculture, fishing, or forestry (AFF),
- The standardized morbidity ratio,
- The projections of the longitude and latitude of the area centroid, and the “position” of each county expressed as a list of adjacent counties.

356

County No. $i$	Obs Cases $Y_i$	Exp Cases $E_i$	Prop AFF	SMR	Project N (km)	Project E (km)	Adjacent Counties
1	9	1.4	0.16	6.43	834.7	162.2	5,9,19
2	39	8.7	0.16	4.48	852.4	385.8	7,10
3	11	3.0	0.10	3.67	946.1	294.0	12
4	9	2.5	0.24	3.60	650.5	377.9	18,20,28
5	15	4.3	0.10	3.49	870.9	220.7	1,12,19
6	8	2.4	0.24	3.33	1015.2	340.2	Island
7	26	8.1	0.10	3.21	842.0	325.0	2,10,13,16,17
8	7	2.3	0.07	3.04	1168.9	442.2	Island
9	6	2.0	0.07	3.00	781.4	194.5	1,17,19,23,29
...							
47	2	5.6	0.01	0.36	640.8	277.0	24,31,46,48,49,53
48	3	9.3	0.01	0.32	654.7	282.0	24,44,47,49
49	28	88.7	0.00	0.32	666.7	267.8	38,41,44,47,48,52,53,54
50	6	19.6	0.01	0.31	736.5	342.2	21,29
51	1	3.4	0.01	0.29	678.9	274.9	34,38,42,54
52	1	3.6	0.00	0.28	683.7	257.8	34,40,49,54
53	1	5.7	0.01	0.18	646.6	265.6	41,46,47,49
54	1	7.0	0.01	0.14	682.3	267.9	34,38,49,51,52
55	0	4.2	0.16	0.00	640.1	321.5	18,24,30,33,45,56
56	0	1.8	0.10	0.00	589.9	322.2	18,20,24,27,55

357

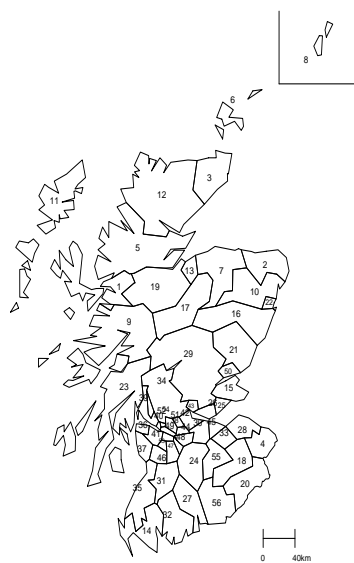


Figure 43: Labels for 56 counties of Scotland.

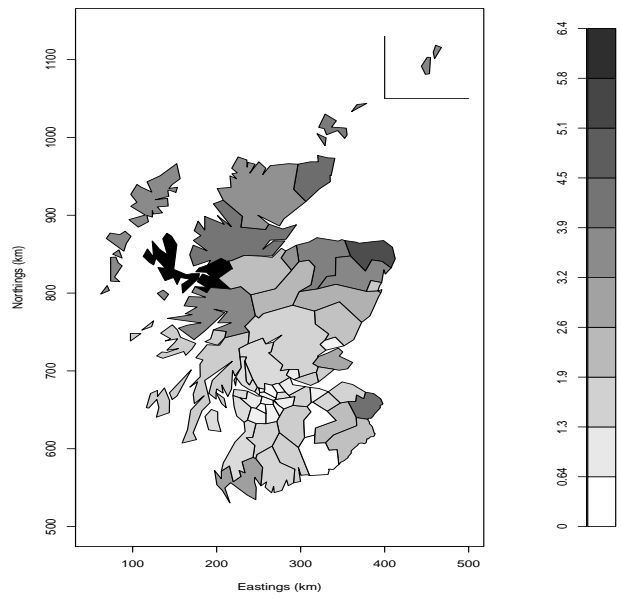


Figure 44: SMRs for male lip cancer in 56 counties of Scotland.

359

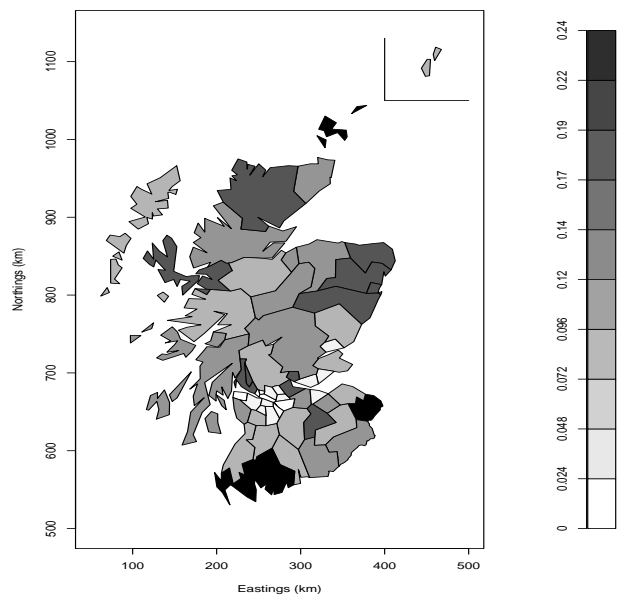


Figure 45: Map of proportion of individuals in agriculture, fishing and farming, for 56 counties of Scotland.

360

## Inference for Spatial Regression

We may extend the GLMM approaches to the spatial setting.

Inference may then proceed via likelihood or Bayesian methods.

Suppose we have data  $Y_i$  with spatial location  $\mathbf{s}_i$  (latitude and longitude, for example), along with covariates  $\mathbf{x}_i$ ,  $i = 1, \dots, n$ . An obvious GLMM is then

*Random Component:*  $Y_{ij}|\theta_{ij}, \alpha \sim p(\cdot)$  where  $p(\cdot)$  is a member of the exponential family, that is

$$p(y_i|\theta_i, \alpha) = \exp[\{y_i\theta_i - b(\theta_i)\}/a(\alpha) + c(y_i, \alpha)],$$

for  $i = 1, \dots, m$  locations.

361

*Systematic Component:* If  $\mu_i = E[Y_i|\theta_i, \alpha]$  then we have a link function  $g(\cdot)$ , with

$$g(\mu_i) = \mathbf{x}_i\boldsymbol{\beta} + \delta_i,$$

so that we have introduced random effects into the linear predictor. The above defines the *conditional* part of the model. The spatial effects are then assigned a distribution, and in a spatial setting it is natural to assume

$$\boldsymbol{\delta} = (\delta_1, \dots, \delta_n)^T \sim_{iid} N_n(\mathbf{0}, \boldsymbol{\Sigma}),$$

where  $\boldsymbol{\Sigma} = \boldsymbol{\Sigma}(\boldsymbol{\alpha})$  is an  $n \times n$  covariance matrix. We also have

$$\text{var}(Y_i|\theta_i, \alpha) = \alpha v(\mu_i).$$

362



## Covariance Models

Many choices are available for the variance-covariance model  $\Sigma$ . A simple choice has

$$\Sigma_{ij} = \sigma_\delta^2 \exp(-\phi \| \mathbf{s}_i - \mathbf{s}_j \|),$$

for  $i, j = 1, \dots, m$ , with  $\sigma_\delta^2, \phi > 0$ . This model is *isotropic* since the covariance only depends on the distance between points.

Obvious links with the AR(1) models we considered in longitudinal data analysis (but here we have no replication over units).

It is sometimes useful to think of the  $\delta_i$ 's as arising from a Gaussian Random Field (GRF). Specifically, a random field  $\delta(\mathbf{s}) \in R^2$  is a (bivariate) Gaussian random field if  $\delta(\mathbf{s}_1), \dots, \delta(\mathbf{s}_n)$  is multivariate normal for any  $\mathbf{s}_i \in R^2$ ,  $i = 1, \dots, n$ . This allows us to do prediction to arbitrary locations.

An obvious extension to the linear predictor is to add independent and identically random effect also. For example, we might fit the model

$$g(\mu_i) = \mathbf{x}_i \boldsymbol{\beta} + \delta_i + \epsilon_i,$$

with  $\epsilon_i \sim_{iid} N(0, \sigma_\epsilon^2)$ ,  $i = 1, \dots, n$ .

363

### Example: Zinc Measurements

For these data a natural starting point is a [Gaussian model](#)

Assume we have data  $Y_i$ ,  $i = 1, \dots, n$  with (possibly after transformation):

$$\mathbf{Y} = (Y_1, \dots, Y_n) \sim N_n(\boldsymbol{\mu}, \boldsymbol{\Sigma})$$

where  $\boldsymbol{\mu} = \boldsymbol{\mu}(\boldsymbol{\beta}) = (\mu_1, \dots, \mu_n)$  with regression parameters  $\boldsymbol{\beta}$  and  $\boldsymbol{\Sigma} = \boldsymbol{\Sigma}(\boldsymbol{\alpha})$  is an  $n \times n$  variance-covariance matrix, with parameters  $\boldsymbol{\alpha}$ .

Hence we have log-likelihood

$$l(\boldsymbol{\beta}, \boldsymbol{\alpha}) = -\frac{1}{2} \log |\boldsymbol{\Sigma}| - \frac{1}{2} (\mathbf{Y} - \boldsymbol{\mu})^T \boldsymbol{\Sigma}^{-1} (\mathbf{Y} - \boldsymbol{\mu}).$$

In general, there are not closed form estimators.

364

## Covariance Models

With a nugget effect  $\sigma_\epsilon^2$  we have

$$\boldsymbol{\Sigma} = \sigma_\epsilon^2 \mathbf{I} + \sigma_\delta^2 \mathbf{R}$$

where  $\mathbf{I}$  is the  $n \times n$  identity matrix, and  $\mathbf{R}$  is an  $n \times n$  correlation matrix.

We have already seen the common spatial exponential model with correlations

$$R_{ij} = \exp(-d_{ij}\phi)$$

and  $d_{ij} = |\mathbf{s}_i - \mathbf{s}_j|$ .

365

## GeoR Example: Modeling of zinc concentration

Figure 46 was created using the following code, and removes the linear effects of distance and elevation from the log zinc measurements:

```
> binzinc <- variog(geozinc,uvec=seq(0,5000,250),trend=~meuse$dist+meuse$elev)
> plot(binzinc)
```

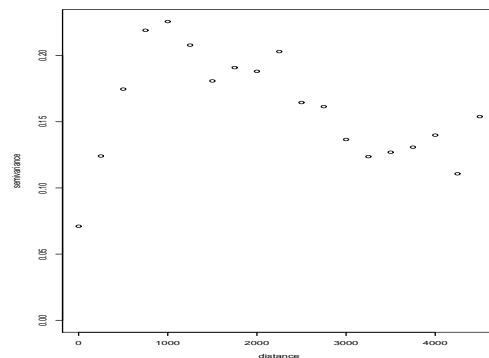


Figure 46: Binned variogram for the log zinc data, after removal of distance from river and elevation covariates effect.

366

Figure 47 was created using the following set of code:

```
> olsfit <- variofit(binzinc,ini=c(.2,500),weights="equal")
> wlsfit <- variofit(binzinc,ini=c(.2,500))
> mlfit <- likfit(geozinc,ini=c(.2,224),trend=~meuse$dist+meuse$elev)
> mlfit
      beta0      beta1      beta2      tausq      sigmasq      phi
" 8.6162" " -2.1072" " -0.2690" " 0.0010" " 0.2065" "241.1982"
likfit: maximised log-likelihood = -54.66
> remlfit<-likfit(geozinc,ini=c(.55,224),method="RML",trend=~meuse$dist+meuse$elev)
> remlfit
      beta0      beta1      beta2      tausq      sigmasq      phi
" 8.6396" " -2.1215" " -0.2701" " 0.0061" " 0.2248" "289.1468"
likfit: maximised log-likelihood = -52.85
> plot(binzinc,max.dist=3000)
> lines(olsfit,max.dist=3000)
> lines(wlsfit,max.dist=3000,lty=2)
> lines(mlfit,max.dist=3000,lty=3)
> lines(remlfit,max.dist=3000,lty=4)
> legend(1500,.075,legend=c("OLS","WLS","ML","REML"),lty=c(1,2,3,4),bty="n")
```

367

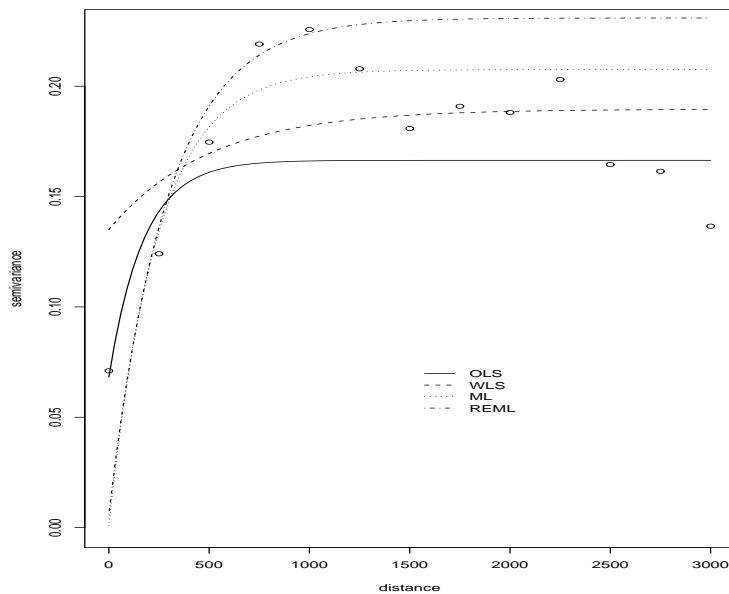


Figure 47: Binned variogram with fitted models.

368

## Prediction of a Spatial Surface

We now describe how to construct a predicted spatial surface for a continuous variable. We construct on a geostatistical technique known as **kriging**, which has many flavors.

Consider the model

$$Y_i = \mathbf{x}_i\boldsymbol{\beta} + \delta_i + \epsilon_i$$

for the observed data  $Y_1, \dots, Y_n$ . We have a noisy version of a spatial process.

We suppose that we would like to predict the underlying spatial surface,  $S_0$ , at a location  $\mathbf{s}_0$ .

Hence we wish to predict

$$S_0 = \mathbf{x}_0\boldsymbol{\beta} + \delta_0$$

where  $\delta_0$  is the spatial random effect associated with location  $\mathbf{s}_0$ .

We have seen that an optimal estimator is:

$$\tilde{S}_0 = E[S_0|\mathbf{Y}]$$

To get specific forms we need to have a more detailed model.

369

Consider the model

$$Y_i = \mathbf{x}_i\boldsymbol{\beta} + \delta_i + \epsilon_i$$

where  $U_i$  are spatial effects with  $\boldsymbol{\delta} = (\delta_1, \dots, \delta_n) \sim N_n(\mathbf{0}, \sigma_\delta^2 \mathbf{R})$  and  $\epsilon_i \sim_{iid} N(0, \sigma_\epsilon^2)$ .

Then we have

$$\begin{bmatrix} S_0 \\ \mathbf{Y} \end{bmatrix} \sim N_{n+1} \left( \begin{bmatrix} \mathbf{x}_0\boldsymbol{\beta} \\ \mathbf{x}\boldsymbol{\beta} \end{bmatrix}, \begin{bmatrix} \sigma_\delta^2 & \sigma_\delta^2 \mathbf{R}_0^\top \\ \sigma_\delta^2 \mathbf{R}_0 & \sigma_\epsilon^2 \mathbf{I} + \sigma_\delta^2 \mathbf{R} \end{bmatrix} \right)$$

where  $\mathbf{R}_0$  is an  $n \times 1$  column vector with  $i$ -th entry describing the correlation between locations  $\mathbf{s}_0$  and  $\mathbf{s}_i$ ,  $i = 1, \dots, n$ .

Then, using properties of the multivariate normal distribution

$$\begin{aligned} \tilde{S}_0 = E[S_0|\mathbf{Y}] &= \mathbf{x}_0\boldsymbol{\beta} + \sigma_\delta^2 \mathbf{R}_0^\top (\sigma_\epsilon^2 \mathbf{I} + \sigma_\delta^2 \mathbf{R})^{-1} (\mathbf{Y} - \mathbf{x}\boldsymbol{\beta}) \\ &= \mathbf{x}_0\boldsymbol{\beta} + \sum_{i=1}^n w_i r_i \end{aligned}$$

where  $w_i$  are a set of weights and  $r_i = Y_i - \mathbf{x}_i\boldsymbol{\beta}$  are the set of residuals.

370

Note that if there is no spatial dependence ( $\sigma_\delta^2 = 0$ ) the weights are zero and we only have contributions from  $\mathbf{x}_0$ . The sizes of the weights depend on the proximity of the new location to the  $n$  data points, and on the magnitude of the spatial dependence, in comparison with the non-spatial.

The variance of the prediction is given by

$$\text{var}(\tilde{S}_0) = \sigma_\delta^2 - \sigma_\delta^2 \mathbf{R}_0^T (\sigma_\epsilon^2 \mathbf{I} + \sigma_\delta^2 \mathbf{R})^{-1} \mathbf{R}_0 \sigma_\delta^2$$

The above estimator may also be justified as the best linear unbiased estimator (if the data are not Gaussian then the optimal estimator will not necessarily be linear in the data).

In practice estimates of  $\boldsymbol{\beta}$ ,  $\boldsymbol{\alpha}$  are substituted into the above formulas.

371

### Example: Predictions of log zinc

Figure 48 is the raw data (note the reference box which we carry out prediction over later) and was created using the commands:

```
> points(geozinc,pt.divide="rank.prop")
> abline(h=330000,lty=2);abline(h=332000,lty=2)
> abline(v=179000,lty=2);abline(v=181000,lty=2)
```

Now we detrend the data and then look at the residuals in Figure 49:

```
> lmfit <- lm(geozinc$data~meuse$dist+meuse$elev)
> lmfit
Coefficients:
(Intercept)  meuse$dist  meuse$elev
      8.4845      -1.9600      -0.2607
> detrend <- as.geodata(cbind(geozinc$coords,lmfit$residuals))
> points(detrend,pt.divide="rank.prop")
> abline(h=330000,lty=2);abline(h=332000,lty=2)
> abline(v=179000,lty=2);abline(v=181000,lty=2)
```

372

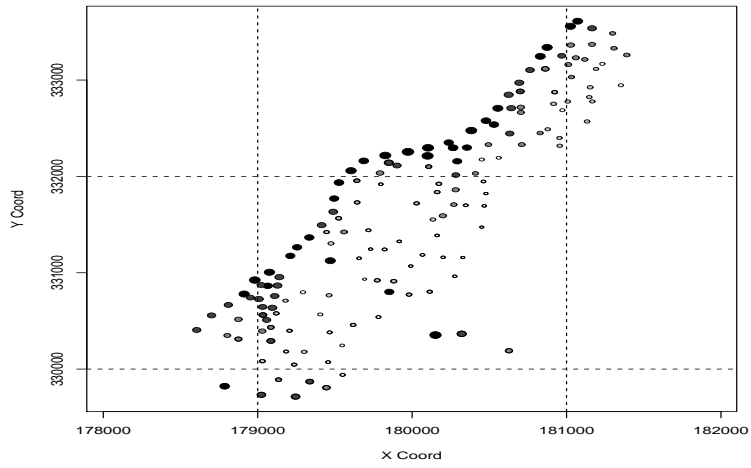


Figure 48: Values of log zinc at sampling locations.

373

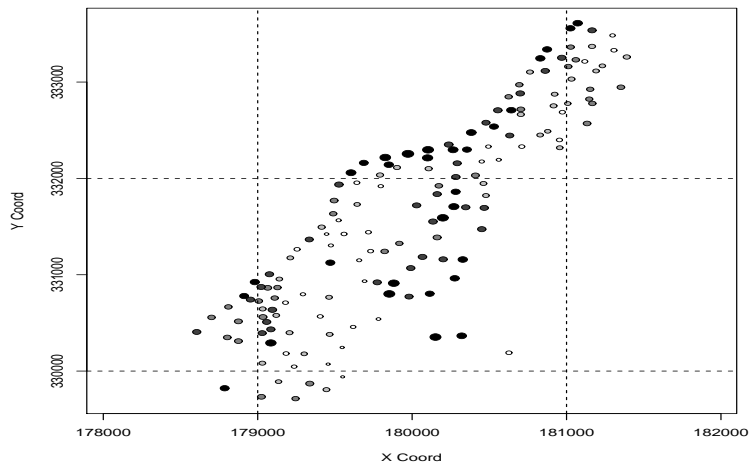


Figure 49: Values of log residuals, after removing effect of distance from river and elevation.

374

Now we carry out Kriging on the residual surface. Figures 50 and 51 show the predicted surface and the standard error surface (note the low standard errors at the sampling points) and were created using the following code:

```
> mlfit2 <- likfit(detrend,ini=c(.2,224))
> mlfit2
      beta      tausq   sigmasq      phi
" 0.0306" " 0.0000" " 0.2076" "238.0914"
likfit: maximised log-likelihood = -54.82
> pred.grid <- expand.grid(seq(179000,181000,l=51),seq(330000,332000,l=51))
> kc <- krige.conv(detrend,loc=pred.grid,krige=krige.control(obj.m=mlfit2))
> image(kc,loc=pred.grid,val=kc$predict,col=gray(seq(1,.1,l=30)))
> image(kc, val=sqrt(kc$krige.var),col=gray(seq(1,.1,l=30)))
```

375

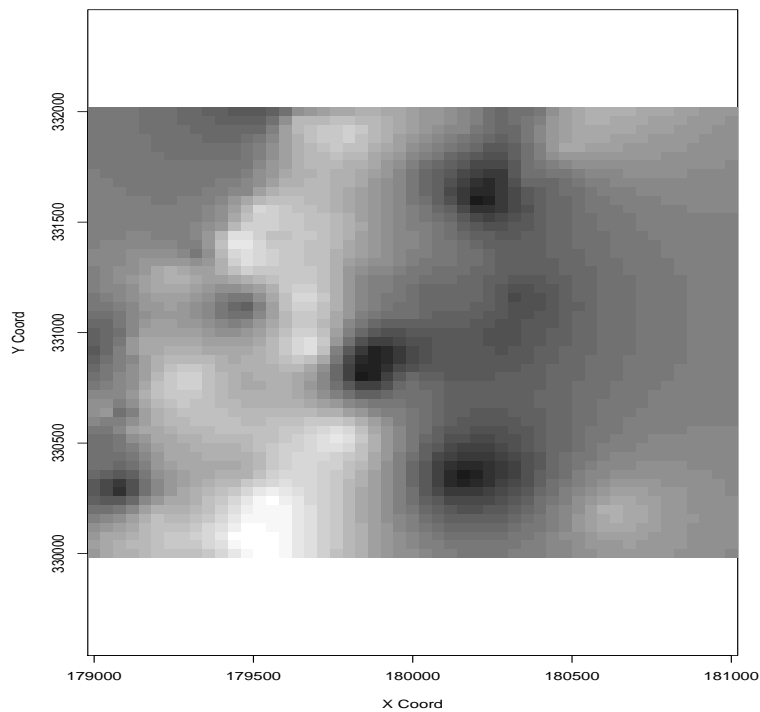


Figure 50: Predicted spatial residual surface.

376

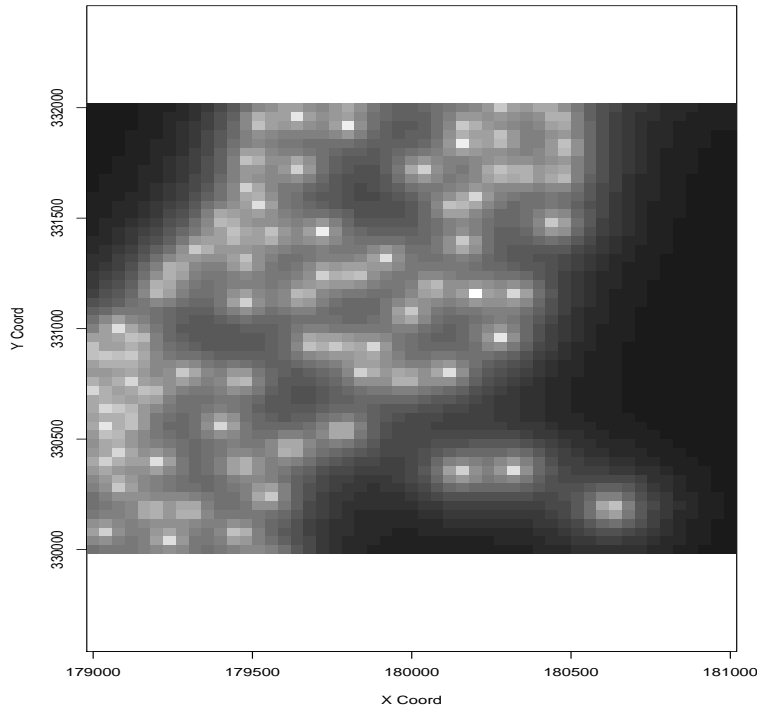


Figure 51: Standard error of prediction of residual.

377

### Childhood Asthma

We carried out a number of regression models from a Bayesian perspective. Table 12 summarizes these analyses for the odds ratio of interest. We consider the model:

- *Stage 1:*

$$Y_i | \mathbf{x}_i, \delta_i \sim \text{Bernoulli}\{p(\mathbf{x}_i, \delta_i)\},$$

for  $i = 1, \dots, n$ , where  $Y_i$  is the case/non-case status,  $\mathbf{x}_i$  is a vector containing the exposure of interest and confounders, and  $\delta_i$  represent unmeasured spatial effect.

- *Stage 2:*

$$\text{logit}\{p(\mathbf{x}, b_i)\} = \mathbf{x}_i \boldsymbol{\beta} + \delta(\mathbf{s}_i),$$

where  $\delta_i = \delta(\mathbf{s}_i)$  is a realization of a GRF.

- *Stage 3:* Priors on  $\boldsymbol{\beta}$  and the parameters of the GRF.

Adjustment for spatial dependence was carried out with covariances between points  $d$  apart being given by  $\sigma_\delta^2 \exp(-d\phi)$ .



The results are almost identical across the different models, all giving evidence of an association between asthma and exposure to traffic.

The prior on  $\phi$  was uniform on (0,50) and the posterior median was 25 with 95% credible interval was 2–49, indicating that the prior has hardly been changed.

The spatial variance parameter  $\sigma_\delta^2$  has posterior median 0.002, again providing evidence that there is no evidence of spatial dependence in the residuals.

Adjust for confounders	Adjustment for spatial	Odds Ratio $\exp(\beta)$	95% Interval
No	No	1.08	0.99–1.20
Yes	No	1.08	0.98–1.20
No	Yes	1.08	0.98–1.19
Yes	Yes	1.08	0.97–1.19

Table 12: Odds ratio summaries (posterior medians and credible intervals) under various models.

379

### Scottish Lip Cancer Data

The individual-level model  $Y_{ij} \sim_{iid} \text{Bernoulli}(e^{\beta_0 + \beta_1 x_{ij}})$  for individual  $i$ ,  $j = 1, \dots, N_i$ , leads to

$$Y_i \sim_{iid} \text{Poisson}(N_i \{(1 - \bar{x}_i)e^{\beta_0} + \bar{x}_i e^{\beta_0 + \beta_1}\}),$$

$i = 1, \dots, m$ .

Random effects can be added to the linear predictor, spatial or non-spatial (or both). Here there is a large change in  $e^{\hat{\beta}_1}$ , because the exposure has spatial structure.

Model	Relative risk	St. Err.
Quasi-likelihood	22.7	7.0
Non-spatial $\epsilon$	22.5	7.8
GRF model ( $\delta$ )	6.3	3.0

Table 13: Estimates and standard errors for individual relative risk,  $e^{\beta_1}$ .

380

For a Bayesian analysis we require a proper prior on  $\alpha_1$ .

Assigning an improper uniform prior to  $\beta_0$  we integrate this parameter from the model to give

$$p(\beta_1|\mathbf{y}) \propto \prod_{i=1}^n \left( \frac{N_i[(1-x_i) + x_i e^{\beta_1}]}{\sum_{i=1}^n N_i[(1-x_i) + x_i e^{\beta_1}]} \right)^{y_i},$$

which tends to the constant

$$\prod_{i=1}^n \left( \frac{N_i(1-x_i)}{\sum_{i=1}^n N_i(1-x_i)} \right)^{y_i} \quad (49)$$

as  $\beta_1 \rightarrow -\infty$ , showing that a proper prior is required. The constant (49) is non-zero unless  $x_i = 1$  in any area with  $y_i \neq 0$ .

The reason for the impropriety is that  $\beta_1 = -\infty$  corresponds to a relative risk of zero, so that exposed individuals cannot get the disease, which is not inconsistent with the observed data unless  $x_i = 1$  in an area (all individuals are exposed), and  $y_i \neq 0$ , in which case clearly the cases are due to exposure. A similar argument holds as  $\beta_1 \rightarrow \infty$  with replacement of  $1-x_i$  by  $x_i$  in (49) providing the limiting constant. Figure 52 illustrates this behavior for the Scottish lip cancer example, for which  $x_i = 0$  in five areas.

381

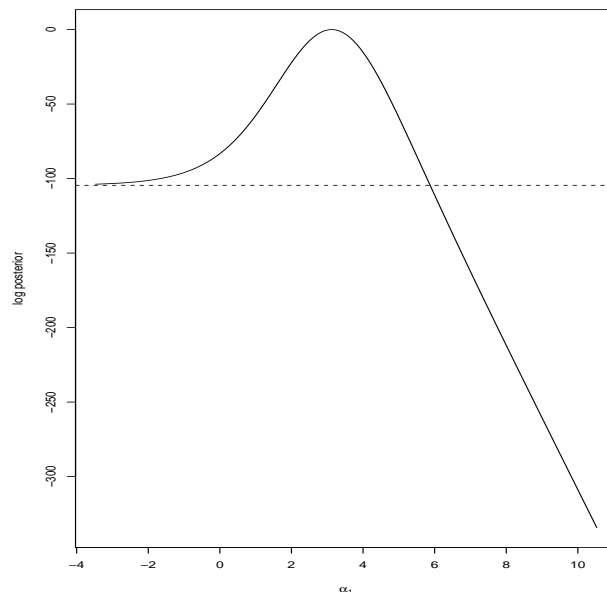


Figure 52: Log posterior for  $\beta_1$  for the Scottish data; the horizontal line is the constant to which this function tends to as  $\beta_1 \rightarrow \infty$ .

382

GeoBUGS has spatial models, and allows maps to be drawn.

```

model
{
  for (i in 1 : N) {
    Y[i] ~ dpois(mu[i])
    log(mu[i]) <- log(E[i]) +
    log( (1-X[i])*exp(beta0) + X[i]*exp(beta0+beta1)) + delta[i]
    mean[i] <- 0
  }
# Multivariate prior distribution for spatial random effects:
  delta[1:N] ~ spatial.exp(mean[], xm[], ym[], tau.delta, phi, 1)
#
# The following prior is derived by assuming there is a 5% chance that corrs
# die to 0.5 in < 5km, and a 95% chance that they die to 0.5 in < 100km.
  dhalf ~ dlnorm(3.107,0.9106)
  phi <- 0.6931/dhalf
  beta0 ~ dflat()
# Prior says 50% RR less than one, 95% less than 50.
  beta1 ~ dnorm(0.0,0.1768)
  tau.delta ~ dgamma(1,0.260)
# Parameters of interest
  base <- exp(alpha0)
  RRx <- exp(alpha1)
}

```

383

```

list(N = 56, Y = c( 9, 39, 11, 9, 15, 8, 26, 7, 6, 20, 13, 5, 3, 8, 17, 9, 2, 7,
  9, 7, 16, 31, 11, 7, 19, 15, 7, 10, 16, 11,5, 3, 7, 8, 11, 9, 11, 8,
  6, 4, 10, 8, 2, 6, 19, 3, 2, 3, 28, 6, 1, 1, 1, 1, 0, 0), E = c(
  1.4, 8.7, 3.0, 2.5, 4.3, 2.4, 8.1, 2.3, 2.0, 6.6, 4.4, 1.8, 1.1,
  3.3, 7.8, 4.6, 1.1, 4.2, 5.5, 4.4, 10.5,22.7, 8.8, 5.6,15.5,12.5,
  6.0, 9.0,14.4,10.2, 4.8, 2.9, 7.0, 8.5,12.3,10.1,12.7, 9.4, 7.2,
  5.3, 18.8,15.8, 4.3,14.6,50.7, 8.2, 5.6, 9.3,88.7,19.6, 3.4, 3.6,
  5.7, 7.0, 4.2, 1.8),X = c(0.16,0.16,0.10,0.24,0.10,0.24,0.10, 0.07,
  0.07,0.16, 0.07,0.16,0.10,0.24, 0.07,0.16,0.10, 0.07, 0.07,0.10,
  0.07,0.16,0.10, 0.07, 0.01, 0.01, 0.07, 0.07,0.10,0.10,
  0.07,0.24,0.10, 0.07, 0.07, 0,0.10, 0.01,0.16, 0, 0.01,0.16,0.16, 0,
  0.01, 0.07, 0.01, 0.01, 0, 0.01, 0.01, 0, 0.01, 0.01,0.16,0.10),
xm = c(
162.1894, 385.7761, 293.9555, 377.9338, 220.6786,340.1739, 324.9915, 442.2445, 194.5176, 367.6924,
112.8916, 247.7566, 289.5922, 227.9563, 342.3574,351.3505, 280.4916, 341.6081, 249.6855, 359.5902,
348.7138, 388.7655, 180.4228, 295.4908, 333.1159,312.0605, 290.1701, 359.4153, 291.3727, 303.4219,
257.4402, 264.9711, 336.4464, 258.0319, 227.1801,234.5294, 218.3428, 279.1010, 235.0805, 254.1736,
250.8301, 287.1202, 292.3773, 288.0333, 320.5682,257.8758, 276.9737, 281.9644, 267.8444, 342.226,
274.8713, 257.8069, 265.5934, 267.8921, 321.4991,322.1780),
ym =c(834.7496, 852.3782, 946.0722, 650.501,870.9356, 1015.154, 842.0317, 1168.904, 781.3746,
828.219, 903.1592, 924.9536, 842.3052, 561.1628,713.0808, 792.1617, 801.0356, 628.6406, 825.8545,
610.6554, 760.2982, 812.7655, 699.6693, 635.7658,701.8189, 691.102, 586.6673, 669.4746, 746.2605,
670.1395, 605.9585, 568.3428, 658.671, 716.452,598.2521, 668.0481, 641.4785, 670.285, 697.044,
677.589, 657.4675, 680.7535, 699.3761, 665.2905,671.6064, 631.046, 640.8285, 654.6629, 666.7073,
736.4561, 678.8585, 683.7104, 646.5754, 682.2943,640.1429, 589.9408))

```

384